

# The effect of in-situ stress parameters and metamorphism on the geomechanical and mineralogical behavior of tunnel rocks

Kadir Karaman\*

Department of Mining Eng., Karadeniz Technical University, 61080 Trabzon, Turkey

(Received May 24, 2023, Revised March 13, 2024, Accepted April 3, 2024)

**Abstract.** Determination of jointed rock mass properties plays a significant role in the design and construction of underground structures such as tunneling and mining. Rock mass classification systems such as Rock Mass Rating (RMR), Rock Mass Index (RMi), Rock Mass Quality (Q), and deformation modulus ( $E_m$ ) are determined from the jointed rock masses. However, parameters of jointed rock masses can be affected by the tunnel depth below the surface due to the effect of the in situ stresses. In addition, the geomechanical properties of rocks change due to the effect of metamorphism. Therefore, the main objective of this study is to apply correlation analysis to investigate the relationships between rock mass properties and some parameters related to the depth of the tunnel studied. For this purpose, the field work consisted of determining rock mass parameters in a tunnel alignment (~7.1 km) at varying depths from 21 m to 431 m below ground surface. At the same excavation depths, thirty-seven rock types were also sampled and tested in the laboratory. Correlations were made between vertical stress and depth, horizontal/vertical stress ratio ( $k$ ) and depth,  $k$  and  $E_m$ ,  $k$  and RMi,  $k$  and point load index (PLI),  $k$  and Brazilian tensile strength (BTS),  $E_m$  and uniaxial compressive strength (UCS), UCS and PLI, UCS and BTS. Relationships were significant (significance level=0.000) at the confidence interval of 95% ( $r = 0.77-0.88$ ) between the data pairs for the rocks taken from depths greater than 166 m where the ratio of horizontal to vertical stress is between 0.6 and 1.2. The in-situ stress parameters affected rock mass properties as well as metamorphism which affected the geomechanical properties of rock materials by affecting the behavior of minerals and textures within rocks. This study revealed that in-situ stress parameters and metamorphism should be reviewed when tunnel studies are carried out.

**Keywords:** contact metamorphism; depth effect; in-situ stress parameters

## 1. Introduction

The geomechanical properties of the rocks are important in the design of geotechnical works such as tunneling, rock slopes, caverns, bridges, silos, building complexes, hill roads, and rail tunnels, etc., and in the classification of rocks for engineering purposes. However, rock type, density, anisotropy, weathering, roughness, moisture content, sample size, etc., can generally affect the geomechanical characteristics of rocks (Karaman and Kesimal 2015a). Additionally, they are dependent on the mineralogy, texture (size, shape, and arrangement of mineral grains, nature of grain-to-grain contacts, and degree of grain interlocking), alteration, and deformation of the rock (Tugrul and Zarif 1999). In geotechnical studies, it is important to investigate the geomechanical properties of the rock mass as well as the rock material. The rock mass classifications form the backbone of the geotechnical works and are widely performed in rock engineering. They constitute the base of the empirical design tool and are commonly used in geotechnical studies and allow better links among appliers, designers, researchers, and engineers.

The rock mass classification systems such as Rock Mass

Quality (Q), Rock Mass Rating (RMR), and Rock Mass Index (RMi) over the last few decades of their development, were performed by many engineers and achieved global recognition (e.g., Palmstrom 1995, Barton 2002, Hoek and Diederichs 2006, Gurocak 2011, Karaman *et al.* 2013).

Tunnel construction is a complex and demanding process that requires careful planning, execution, and monitoring to ensure the successful completion of the project. Geological factors that affect tunnel construction include depth and character of overburden; bedrock surface configuration; rock properties; fabric and type; structural features of the rock mass; occurrence of ground-water and construction under the seabed (Chen *et al.* 2022, Banihashemigargari and Rezaeifarei 2023, Kang *et al.* 2023). Anagnostou (1993) mentioned that large deformation mainly depends on rock strength and overburden thickness, and it can occur in any type of rock mass. Singh *et al.* (1997) pointed out that large deformation occurs on the premise of weak surrounding rock combined with high in-situ stress. Sharma and Judd (1991) reported that more tunnels at lower depths are damaged than those at large depths. Wang *et al.* (2009) studied a method that was developed to evaluate the changes in porosity and bulk modulus with depth (0-160 meters). They showed that the porosity decreases with depth. Chen *et al.* (2012) investigated the influence of the depth of a tunnel on its seismic damage. They indicated the potential damage to a tunnel by an earthquake depends critically on its depth.

---

\*Corresponding author, Associate Professor  
E-mail: kadirkaraman@ktu.edu.tr

Abdou and Mahmoud (2013) evaluated the relationships between shallow depths (1–8 meters) from the surface and rock properties (rock quality designation (RQD) and UCS, and rock recovery (REC)). They reported that REC, RQD, and UCS increase as the depth of the sample below the ground surface increases. Considering the values of the correlation coefficient, they found that there are poor relationships between both REC and RQD with depth, whereas no relationship was obtained between UCS and depth. Bieniawski (1989) stated that longer stand-up times can be achieved by selecting rock reinforcement elements in accordance with some factors such as the depth below the surface (in situ stress), tunnel size and shape, and the method of excavation. Min *et al.* (2004) investigated the relationship between horizontal/vertical stress ratio ( $k$ ) and permeability of rock masses and reported that permeability decreases as the  $k$  ratio increases until the  $k$  ratio reaches approximately 2.5. It is commonly known that rock at depth is subjected to stresses resulting from the weight of the overlying strata and from locked-in stresses of tectonic origin. When an opening is excavated within this rock, the stress field is locally disrupted and a new set of stresses are induced in the rock surrounding the opening. Therefore, knowledge of the magnitudes and directions of these in situ and induced stresses is an essential component of underground excavation design (Brown and Hoek 1978, Sheorey 1994). In addition to the in-situ stress aroused by the earth's crust above the rocks, magma intrusion beneath the rocks causes contact metamorphism, affecting the geomechanical behavior of rocks. Unlike the tunnel rocks, Abioye (2015) reported that as the effect of metamorphism increases, some parameters of outcrop rocks such as the brittleness increase. Additionally, Yan *et al.* (2023) evaluated the contact metamorphic rocks and stated that the previous studies generally ignore the minor components in rock and mineral systems.

According to the literature survey, few researchers reported the effect of in-situ stress parameters and metamorphism on the geomechanical properties of the rocks (Verman *et al.* 1997, Min *et al.* 2004, Chun *et al.* 2009, Wang *et al.* 2009, Abdou and Mahmoud 2013). Therefore, the aim of this study is to investigate the effect of in-situ stress parameters (vertical and horizontal) on the correlations within the geomechanical properties (UCS, PLI ( $I_{s(50)}$ ), RQD, Em, etc.) of the tunnel rocks. In this study, differences affecting the correlations in metamorphic rocks were observed, and the reasons were also investigated in detail in terms of general geology and mineralogy.

## 2. General geology and sampling location

The eastern Black Sea Region is an efficient basin in terms of small hydroelectric powers because of the amount of its falling precipitation and important surface water potential. In addition, many geotechnical studies such as road tunnels and underground mining are carried out in the region. The study area is in the northeast part of the Eastern Pontides Tectonic Belt (Ketin 1966). Being mostly volcanic rocks in the study area (Cambasi), there are four

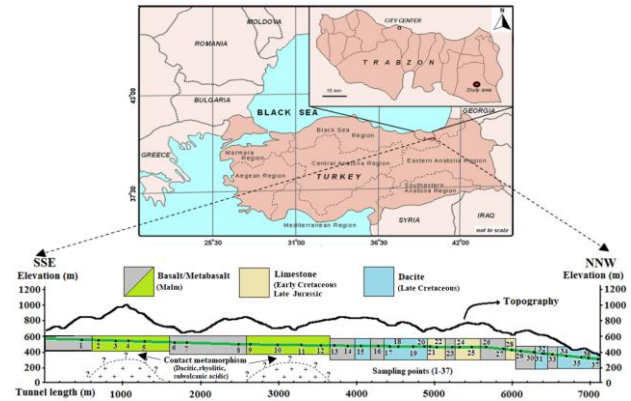


Fig. 1 Location map of the study area (a) and simplified geological cross section through the tunnel (b)

formational groups of rocks identified along the tunnel route. Those are Jurassic (Malm) aged Hamurkesen Formation comprised of mostly metabasalts and basalts at the upstream lengths of the tunnel, Early Cretaceous-Late Jurassic aged Berdiga Formation with reefal, sandy, and cherty limestones, and Late Cretaceous aged Kızılkaya Formation with rhyolite, dacitic lava and pyroclastics. Hamurkesen Formation which shows wide expansion along the studied tunnel alignment is chiefly overlain by the Berdiga Formation. The lithologies of the tunnel route mainly consist of basalt, metabasalt, limestone and dacite. The lowest and the uppermost lithologies belong to the Jurassic (Hamurkesen Formation) and Quaternary (alluvium), respectively (Karaman and Kesimal 2015b).

The field-work consisted of the sampling of 37 excavation faces in Cambasi tunnel (Trabzon) to depths between 21 m to 431 m below ground surface (Fig. 1). When the lithology and discontinuity characteristics changed along the tunnel route, measurements were made on the excavation faces and the representative rock block samples were collected from these points, 24 of which were volcanic, 8 were metamorphic, and 5 were sedimentary. The tunnel is 7132 m long with a cross-sectional area of 24.5 m<sup>2</sup>. The study area offers a rugged morphology. The morphology of the area mainly consists of high mountains, varying from 300 to 1.786 m in height above the sea level, and deep valleys with step walls.

## 3. Experimental studies

### 3.1 Field and laboratory studies

Different parameters were taken into consideration such as depth of rock below ground surface ( $D$ ), deformation modulus of rock masses ( $E_m$ ), RQD, RMR,  $Q$ , and  $RM_i$ . Within this scope, some input parameters were determined as suggested by the rock mass classification systems. An equation ( $E_m = I_{s(50)} \times 10^{(0.01 * RQD - 0.25)}$ ) proposed by Karaman *et al.* (2015) was used for the calculation of the deformation modulus of the rock masses. It is generally believed that the vertical in situ stress in the region is comprised of a simple gravitational gradient based on the

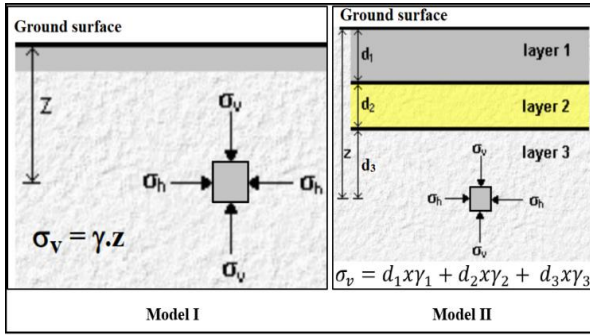


Fig. 2 Vertical stress calculation based upon the mode-I and mode-II

density of the rocks within the stratigraphic section (Corkum *et al.* 2018).

Lithostatic principal stresses are the result of the weight of the materials above which are known as vertical and horizontal stresses. While horizontal stress was calculated from the ratio of horizontal to vertical stress for different deformation modulus based upon Sheorey’s model (Sheorey 1994), vertical stress was determined by using the equations of Mode-I and Mode-II defined in Fig. 2.

### 3.2 Tests performed in the laboratory for rock materials

Each block sample was inspected for macroscopic defects to provide test specimens free from fractures, cracks, partings, or alteration zones. One of the significant parameters affecting the strength of rocks is anisotropy. However, the volcanic rocks show no prismatic, pillow lava, and/ or flow structures. Additionally, the metamorphic rocks (metabasalts) contain no features such as schistosity or foliation that could lead to anisotropy except for one sample (depth = 228 m) which shows some mineralization and alterations. All rock blocks were cored using 54.7-mm-diameter diamond coring bits. UCS, PLI, and BTS tests were performed under the ISRM-suggested method (ISRM 2007). To prepare the core samples, laboratory core drills and sawing machines were used. The digital PLI test apparatus was utilized for testing. The axial point load test method was performed on NX-size core samples. PLI value was corrected to the standard equivalent diameter ( $De$ ) of 50 mm for each test. The value for the PLI (MPa) was determined by the following equation

$$PLI_{(50)} = f(P / De^2) \quad (1)$$

where  $P$  is the failure load,  $De$  is the equivalent core diameter ( $De^2=4A/\pi$  where  $A=WD$ ,  $W$  and  $D$  are the sample size parameters, and  $f$  is the size correction factor  $= (De/50)^{0.45}$ ).

BTS was carried out on a circular disk which was placed between two platens and loaded compression producing a nearly uniform tensile stress distribution. Ten core samples were used to determine the mean BTS value with a diameter to height of 54.7 mm to 27 mm. A loading rate of 200 N/s was applied until sample failures (ISRM 2007). BTS of the rocks was calculated by using the following equation

$$BTS = 2P/\pi Dt \quad (2)$$

where  $P$  is the applied load at failure,  $D$  and  $t$  are the diameter and thickness of the rock sample, respectively.

Core samples that had a length-to-diameter ratio of 2.5 were used for UCS tests. The UCS tests were performed using a servo-controlled testing machine, having a load capacity of 300 tons. The stress rate was applied at 0.75 MPa/s during the tests. The mean UCS value was obtained by averaging the strength values of five tests on the same lithotype/sampling point. A total of 915 test samples were utilized for UCS, PLI, and BTS tests.

### 3.3 Rock mass classifications

The rock mass along the tunnel route is divided into 37 structural regions, and the input parameters for rock mass classification systems are determined for each structural region. The RMR system sustained its development until 1989 based on the observations obtained from a great number of geotechnical projects such as mining, tunnelling, and slope stability (Bieniawski 1989). The six parameters used in RMR are as follows: UCS of intact rock material, RQD, discontinuity spacing, discontinuity conditions, groundwater condition, and discontinuity orientation. Q system was established in 1974 based on 212 tunnel cases (Barton *et al.* (1974)). Q-system and RMR, have been widely used to estimate rock mass behavior and deformability parameters (Barton *et al.* 1974, Zhao *et al.* 2021, Zhou and Yang 2021, Kim *et al.* 2022). The six parameters are united in the following manner to compute the rock-mass quality

$$Q = \left(\frac{RQD}{J_n}\right)\left(\frac{J_r}{J_a}\right)\left(\frac{J_w}{SRF}\right) \quad (3)$$

where RQD has a minimum score of 10,  $J_n$  symbolizes the score of the joint sets number,  $J_r$  is the score for the roughness of the joint surface,  $J_a$  symbolizes the score for the clay filling or alteration degree,  $J_w$  symbolizes the groundwater pressure effects scores and the stress reduction factor (SRF) is the score for faulting, strength and stress ratios in hard rocks and squeezing or swelling.

The rock mass index (RMI) is a volumetric parameter indicating the approximate UCS of a rock mass, it was first presented by Palmstrom (1995). It makes use of the UCS of intact rock and the reducing effect of the joints penetrating the rock (JP) given as

$$RMI = UCS * JP \quad (4)$$

$$JP = 0.2\sqrt{jC(Vb)^{Db}} \quad (5)$$

$$jC = jL \frac{jR}{jA} \quad (6)$$

$$Db = 0.37 jC^{-0.2} \quad (7)$$

The symbols in the expressions above represent: UCS; Uniaxial compressive strength of intact rock, JP; Jointing parameter,  $jC$ ; Joint condition factor,  $Vb$ ; Block volume, measured in  $m^3$ ,  $jL$ ; Joint size,  $jR$ ; Joint roughness.



Fig. 3 Some examples of field and laboratory studies; a tunnel face (a), measurements of orientation by compass (b), measurements of roughness by profilometer (c), core samples from a tunnel face (d), PLI test (e), BTS test (f), core trimming (g) some samples for PLI and BTS (h) and UCS tests (i)

Rock material and rock mass parameters along with minimum, maximum, and mean values are summarized in Table 1. Some examples of field and laboratory studies are given in Fig. 3.

#### 4. Result and discussion

Figs. 4 and 5 show the relationships between the depth of the sample below the ground surface (Depth,  $D$ ) and the properties of the rock mass ( $RMi$ ,  $Q$ ,  $RMR$  and  $Em$ ). All rocks (37 samples) included in the correlation analysis had scattered points. Considering the scattered points and correlation analysis, there were no statistically significant relationships (sig. level  $> 0.05$ ) between depth and other parameters ( $RMi$ ,  $Q$ ,  $RMR$ , and  $Em$ ) for all rocks (Fig. 4). Jiang *et al.* (2009) determined the fracture normal stiffness, including the data of deformation modulus of the rock masses and depth values which were obtained from a well.

They (Jiang *et al.* 2009) reported a good nonlinear relationship between deformation modulus (1.2-13.3 GPa) and depth (10-140 m). Unlike the well data, this study was carried out in a tunnel where rock mass properties could be measured in large-scale excavation faces, and in-situ stresses were taken into account. In concordance with the current study, Chun *et al.* (2009) found a weak correlation ( $R^2=0.32$ ) between deformation modulus (3.9–45 GPa) and depth (4–166 m).

The relationships between the rock mass properties and the depth may indicate more meaningful results when the rock type (i.e., basalt only) is studied. Therefore, correlation analyses were performed based on the rock types (Dacite (D), Limestone (L), Basalt (B), and Metabasalt (M)) instead of all rocks/depths (Figs. 5(a)-5(d)). From these figures, generally, it can be noticed that  $Em$ ,  $RMi$ ,  $Q$ , and  $RMR$  values increase as the depth increases. The correlation coefficients on the relationships between depth with  $Em$ ,

Table 1 Engineering properties of rock material and rock masses

	Related Properties	Min.	Max.	Average
All rocks N:37	Depth (m)	21.4	430.5	256.0
	RMR	43.0	74.4	60.3
	Q	1.8	14.9	10.1
	RMi	1.1	8.8	3.7
	Em (GPa)	6.0	38	18.8
	$\sigma_v$ (MPa)	0.6	11.6	6.9
	$\sigma_H$ (MPa)	1.5	14.2	6.5
	UCS (MPa)	34	197	95
	PLI (MPa)	2.8	10.0	5.4
	BTS (MPa)	4.4	34.4	14.6
Metabasalt N:8	Depth (m)	228	430.5	317.5
	RMR	55.5	73.1	67.5
	Q	7.6	14.93	13.3
	RMi	2.52	8.12	4.54
	Em (GPa)	14.4	33.3	24.01
	$\sigma_v$ (MPa)	6.2	11.6	8.6
	$\sigma_H$ (MPa)	5.3	14.2	8.9
	UCS (MPa)	66	158	108
	PLI (MPa)	3.8	8.8	6.5
	BTS (MPa)	9.4	26.3	18.1
Limestone N:5	Depth (m)	193.9	292.8	242.8
	RMR	43	65.6	58.48
	Q	2.23	10.8	8.84
	RMi	1.09	5.79	3.59
	Em (GPa)	13.7	20.2	17.96
	$\sigma_v$ (MPa)	5.2	7.9	6.6
	$\sigma_H$ (MPa)	5.0	6.5	5.9
	UCS (MPa)	75	120	99
	PLI (MPa)	5.2	5.7	5.5
	BTS (MPa)	10.8	18.0	14.0
Dacite N:11	Depth (m)	21.4	407.2	204.6
	RMR	49.7	68.9	57.06
	Q	1.75	14.76	7.93
	RMi	1.24	5.64	3.03
	Em (GPa)	9.6	21.9	13.55
	$\sigma_v$ (MPa)	0.6	9.3	5.1
	$\sigma_H$ (MPa)	1.5	6.4	4.8
	UCS (MPa)	56	132	79
	PLI (MPa)	3.3	6.8	4.1
	BTS (MPa)	5.3	20.6	10.7
Basalt N:13	Depth (m)	137	393.8	268.52
	RMR	48	69.7	58.51
	Q	7.6	14.93	10.33
	RMi	1.26	8.78	3.53
	Em (GPa)	9.6	31.5	20.10
	$\sigma_v$ (MPa)	3.7	10.6	7.3
	$\sigma_H$ (MPa)	4.4	11.3	7.1
	UCS (MPa)	34	197	105
	PLI (MPa)	2.8	10	6.1
	BTS (MPa)	4.4	34.4	16.8

$RMi$ ,  $Q$ , and  $RMR$  are considered to be very strong as shown in Figs. 5(a)-5(d). However,  $RMR$  is less affected by depth than others. It can be attributed to the discontinuity which directly affects the rock mass parameters of  $Em$ ,  $RMi$ , and  $Q$  compared to  $RMR$  which had a water effect of 15%. Verman *et al.* (1997) reported that the deformation modulus of the rock mass increases with an increase in  $RMR$  and the tunnel depth due to the effect of the confining

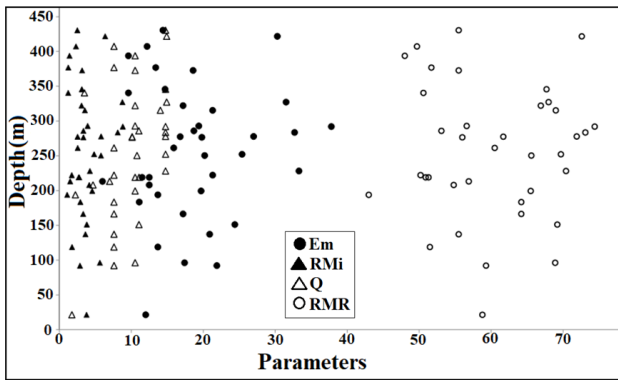


Fig. 4 Relationships between rock mass classifications and depth

pressure. Chun *et al.* (2009) revealed that the confining stress increases with increasing depth, which will cause the closure of the fractures in the rock mass. The degree of contact between the rock masses will then increase the deformation modulus. The reason behind the poor relationships between rock mass properties and the depth for all rocks is due to the different rock samples (dacite, limestone, etc.) having different characteristics (mineralogy, density, discontinuity spacing, and aperture, etc.). The average unit weight was found as 26.77 kN/m<sup>3</sup> for all rock types, varying from 24.62 and 30.51 kN/m<sup>3</sup>. Fig. 6(a) shows the relation between values of depth below the surface and vertical stress for all rocks taken from the 37 excavation faces. These results were consistent with the findings of Brown and Hoek (1978). Vertical stress was also calculated using mode-I (Fig. 6(a)) and mode-II (Figs. 6(a) and 6(b)) described in Fig. 2 for the rocks of excavation faces didn't have unique lithology (for 14 rock types). Since most of the rocks have unit weight values between 25–28 kN/m<sup>3</sup>, vertical stress values were similar for mode-I and mode-II. The mean percentage difference between mode-I and mode-II for 14 points was lower than 1% (0.94).

Overburden at the tunnel section of the Cambasi varies from 21.4 to 430.5 m, which gives vertical gravitational stress magnitude ranging from 0.6 to 11.6 MPa and the horizontal stress varying from 1.5 to 14.2 MPa (Fig. 7). Moomivand *et al.* (2022) reported that vertical stress can be estimated using depth and unit weight because the estimating vertical stress obtained by multiplying the unit weight by the thickness of the overburden is approximately the same as vertical stress test results based on the analysis of 1041 unit weight test results of different types of rocks. However, the authors stated that the estimated horizontal-to-vertical stress ratio (k) obtained from four different previous methods was significantly different from one method to another. The horizontal stresses acting on an element of rock at a depth below the surface are much more difficult to estimate than the vertical stresses. In the current study, horizontal stress values were obtained from the ratio of horizontal to vertical stress (k) for different deformation moduli based on Sheorey's Equation (Sheorey 1994).

Bieniawski (1989) found that for a depth of 120 ft, the vertical stress is calculated as 132 psi which gives the horizontal-to-vertical stress ratio as 3.4. Brown and Hoek (1978) and Herget (1988) indicate the horizontal stresses at

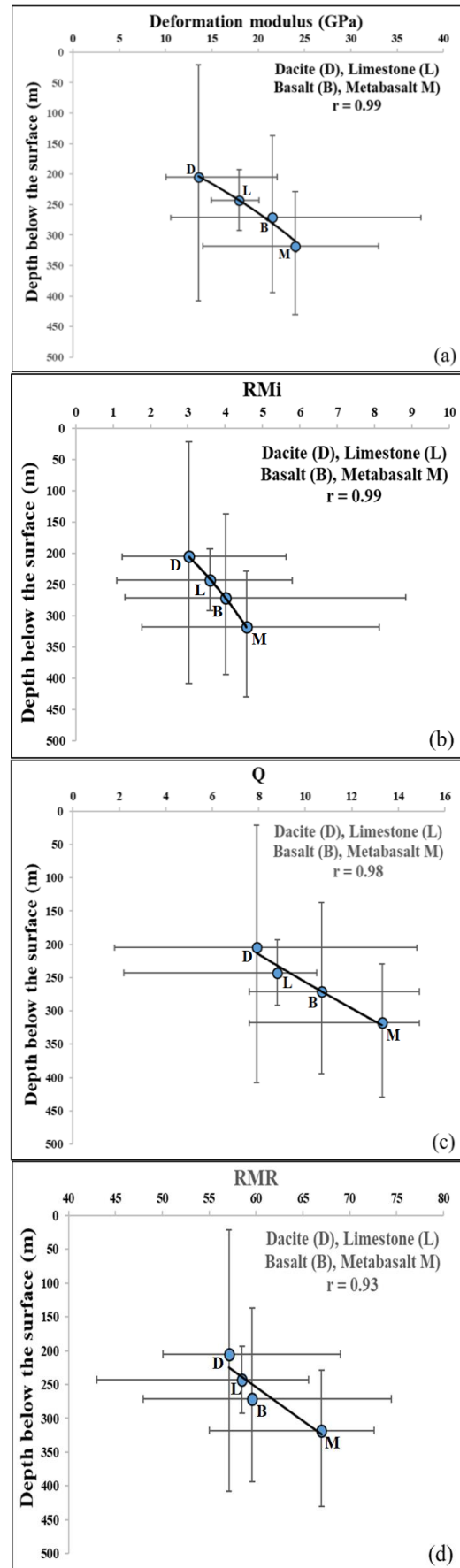
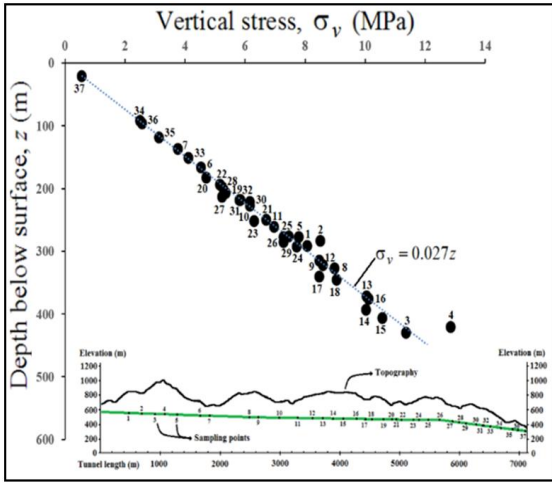
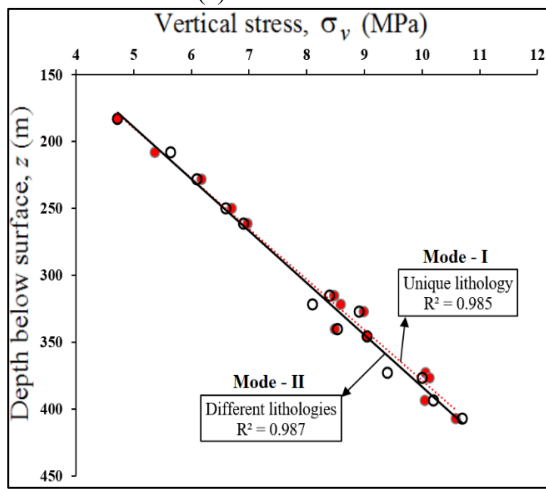


Fig. 5 Relationships between rock mass parameters and depth (a)-(d)



(a) for all rocks



(b) for mode-I and mode-II

Fig. 6 Relations between vertical stress and depth

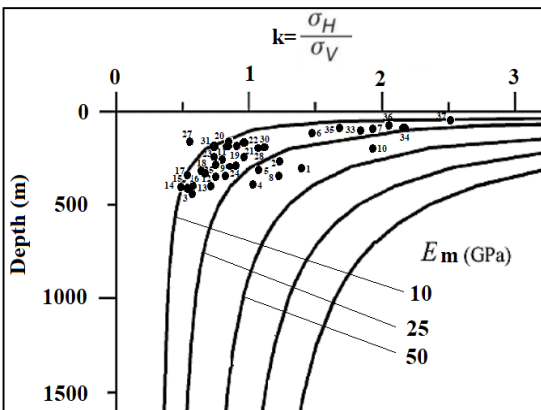


Fig. 7 Relation between horizontal/vertical stress ratio (k) and depth

civil and mining sites around the world show that the k ratio tends to be high at shallow depth and that it decreases at depth. K ratios were varied from 0.47 to 2.49 which is consistent with the literature in terms of the higher k at shallow depth. In this regard, Bird (1942) describes bursts at less than 150 m depth during tunneling in massive granites. Parker (1966) found the average horizontal stress

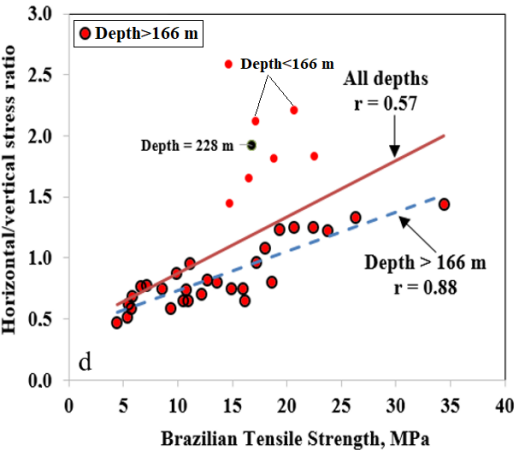
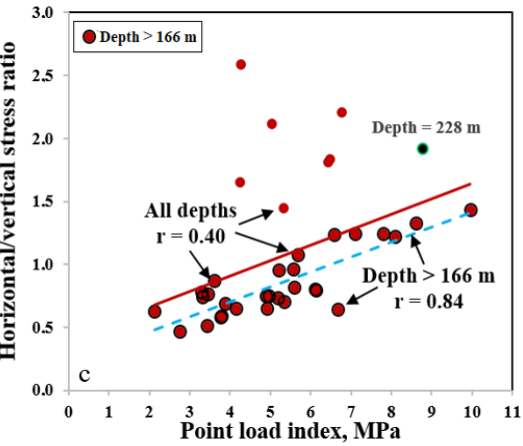
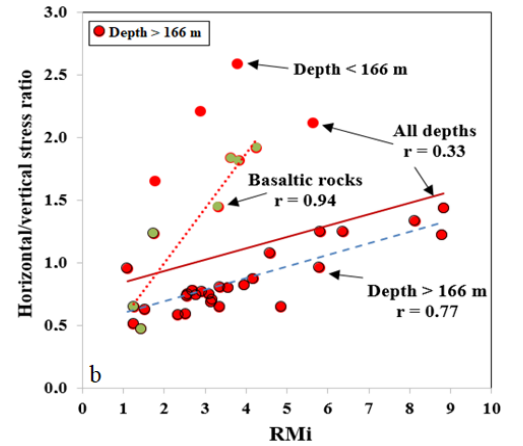
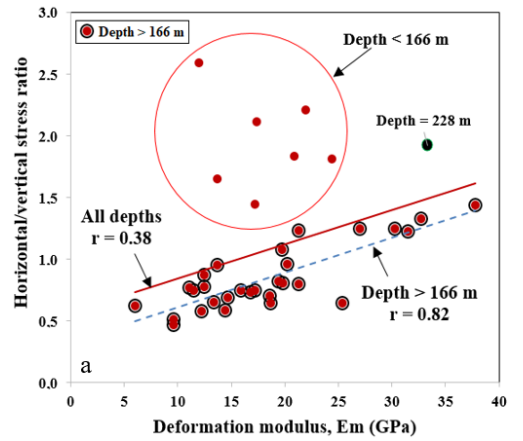


Fig. 8 Relations between k ratio with deformation moduli (a), Rmi (b), PLI (c) and (BTS) (d)



Fig. 9 Tunnel excavation face related to metabasalt and core samples

as 13.8 MPa at a depth of 150 m. The average horizontal stress value of this depth was obtained as about 8 MPa in this study.

New correlations were tried to find out the effect of the depth factor on the geomechanical properties, taking into account the ratio of the horizontal and vertical stress ( $k$ ) (Figs. 8(a)-8(d)). It was shown in the correlations that the  $k$  values for depths lower than 166 meters generally exhibited high fluctuations. Relatively strong relations ( $r$ : 0.77–0.88) with sig. levels of 0.000 were obtained between the data pairs at depths higher than 166 meters (Figs. 8(a)-8(d)). Notwithstanding that, relatively weak correlation coefficients ( $r$ : 0.33–0.57) with sig. levels of 0.000–0.045 were obtained between the  $k$ – $Em$ ,  $k$ – $RMi$ ,  $k$ – $PLI$ , and  $k$ – $BTS$  for all depth values. Although the relations were significant statistically, the sig. level of correlation is approximately at the statistical limit of confidence interval value ( $\alpha=0.05$ ) for all depths. Lower correlations could be ascribed to the high horizontal stress at shallow depths. Notwithstanding that strong relation was obtained between  $k$  and  $RMi$  for some basaltic rocks ( $r=0.94$ ). Min *et al.* (2004) reported that the pure elastic and the elastoplastic models show a similar response until the stress ratio,  $k$  reaches approximately 2.5 and this stress ratio agrees well with the critical stress ratio (2.45). Therefore, in this study, another reason for lower correlations between  $k$  and geomechanical properties of all rocks may be  $k$  values which are close to 2.5 related to shallow depth (<166 m).

Rocks that differ in mineral composition, porosity, cementation, consolidation, texture, and structural anisotropy can be expected to have different strength and deformation properties. Solid constituents are mainly considered for the geological nomenclature of rocks, whereas from the engineer's point of view, pores, defects, and anisotropy are of greater mechanical significance (Franklin 1970, Karaman and Bakhytzhah 2020). Therefore, the mechanical properties can vary even if the rock name is the same. Karaman and Kesimal (2015a) reported that unit weight and porosity are some of the important parameters that affect both UCS and P wave velocity values of rocks. In the current study, the porosity values of rocks were mostly lower than 2%. In addition to the critical depth value

determined in this study, findings obtained at the depth of 228 meters were mostly different from the others (Fig. 9). Therefore, mineralogical thin section and polished section analyses were conducted to understand the reason both for metabasalt at the depth of 228 m and other metabasalts (Figs. 10(a)-10(f)). According to the thin section analyses, all metabasalts are composed primarily of chlorite, epidote, secondary quartz, pyrite, amphibole, and chloritized amphibole minerals. However, the metabasalt at the 228th meter contains more intense mineralization. Additionally, the mineral grain sizes (varying sizes, large and small) of the metabasalt at the 228th meter vary between 200–1000  $\mu\text{m}$  whereas the grain sizes (generally equal-sized microcrystals) of the other metabasalts range from 30 to 150  $\mu\text{m}$ , with an average of around 50  $\mu\text{m}$ . Unlike the metabasalt at the 228th m, the micro-veins within the rocks provide a structure integrated with the rock for other metabasalts (Figs. 10(c) and 10(d)). Polished section analyses were performed to determine the type of the opaque mineral and to examine its grain sizes (Figs. 10(e) and 10(f)). Polished section analyses indicate that the metabasalts have pyrite content in the rock of about 1–2.13% when all sections are examined. However, pyrite minerals are concentrated in places where the fractures in the rock are dense and are found in a small amount, heterogeneously dispersed in other parts of the rock. Therefore, pyrite content in heavy fractured zones was obtained as 5.2% when analyzing one image area using the CLEMEX image analysis system. Similar to the thin section analysis results, in the polished section analysis, pyrite minerals were seen in equal-sized and small grains in other metabasalts, and varying sizes in the metabasalt at the 228th m. Bulut and Tarhan (1992) mentioned that volcanic intrusion cuts across the basalt and metabasalt units in the study area. Pluton intrusion will inevitably lead to contact metamorphism of the surrounding geological bodies (Sklyarov *et al.* (2020). Mineralogical thin and polished section analyses indicate that basalts turned into metabasalts with the effect of low-grade contact metamorphism. However, metabasalt at the 228th m was more affected by contact metamorphism and changed its mineral structure, thus causing the difference in geomechanical properties. It is commonly known that alteration and weathering adversely affect the geomechanical behavior of rocks. Similarly, Karaman *et al.* (2019) observed a negative relation ( $r=-0.69$ ) between UCS and pyrite content.

Kahraman (2001) made correlations between  $PLI$  and  $UCS$  for coal-measure rocks and other rocks without considering the depth effect and indicated two separate trends, one for the coal-measure rocks and another for the other rocks. Similarly, correlation coefficients were different for the rocks at two depths considered. Figs. 11(a)-11(c) illustrates the relationships between  $UCS$  with  $Em$ ,  $PLI$ , and  $BTS$  prepared from rock samples taken from 37 excavation faces for all depths and depths > 166 meters. As expected, the  $UCS$  values increased with increasing the  $Em$ ,  $PLI$ , and  $BTS$  for the rock samples obtained from all depths and depths > 166 meters of the tunnel. The variation of correlation coefficients between the data pairs at all depths

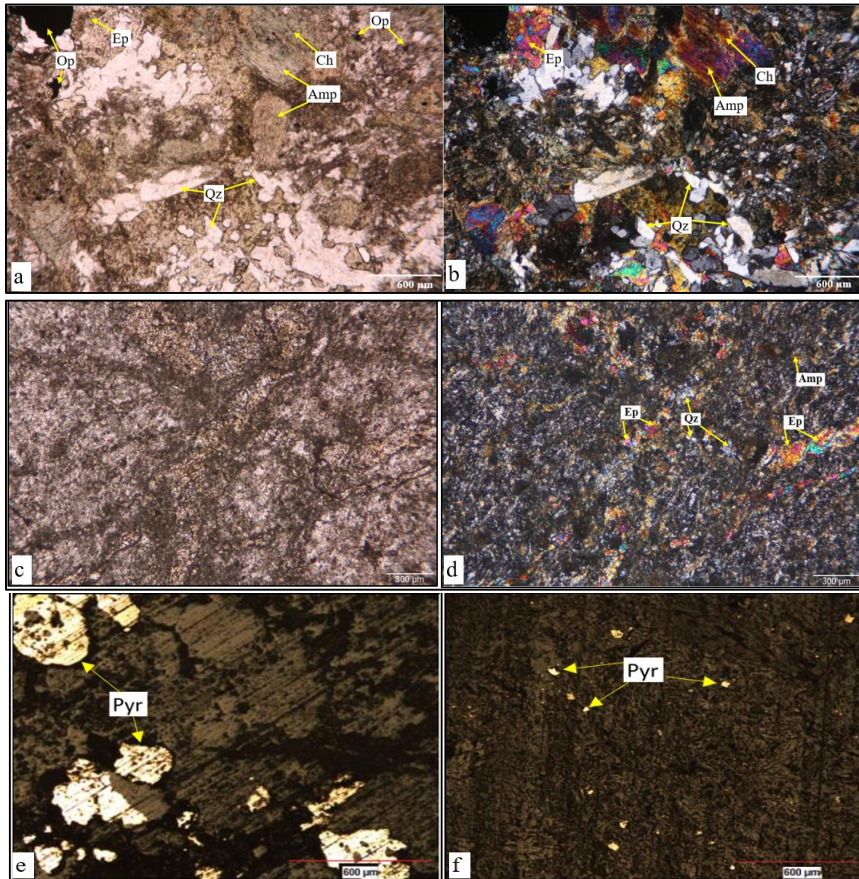
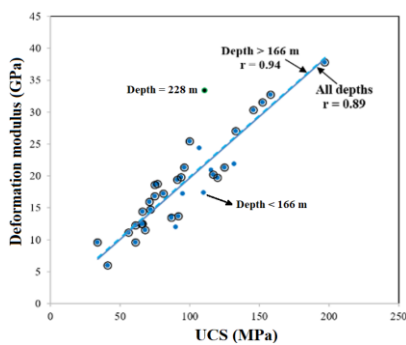
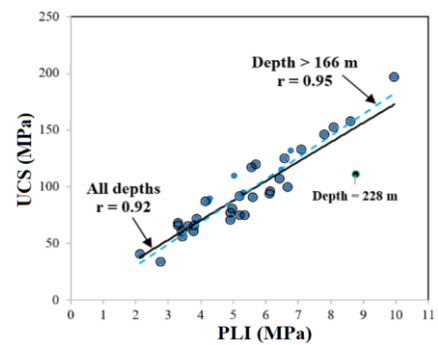


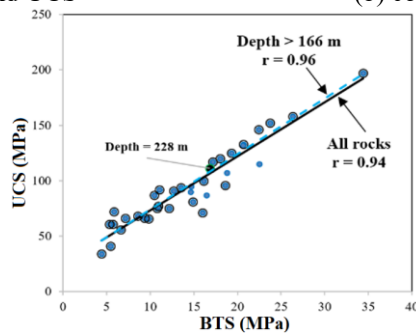
Fig. 10 Microscopic thin section images of metabasalt at depth 228 m (plane-polarized light, a and cross-polarized light, (b) and other metabasalts (plane-polarized light, c and cross-polarized light, (d), and polished section images of metabasalt at depth 228 m (e) and other metabasalts (f), Ep: Epidote, Qz: Quartz, Amp: Amphibole, Ch: Chlorite, Op: Opaque mineral (pyrite), Pyr: Pyrite



(a) correlation between Em and UCS



(b) correlation between UCS and PLI



(c) correlation between UCS and BTS

Fig. 11 Relationships within some familiar rock parameters based on the depth

and depths higher than 166 meters was determined to vary in the range of 0.89–0.94 and 0.94–0.96, respectively. In this regard, it can be mentioned that in situ stress parameters as a result of the tunnel depth below the surface may relatively affect relationships between the geomechanical properties of rocks.

Some researchers reported that correlations can be affected by some factors such as the type and characteristics of the rock studied, the range of dataset used, and the test type (Kahraman 2001, Yagiz 2009, Karaman and Bakhytzhan 2020). In addition to these factors, it is revealed in this study that the in situ stress parameters linked to depth below the surface can be considered as an indirect factor that affects the correlations. It is therefore suggested that limitations about the correlation analyses should be considered at the design stage of the projects with caution for rocks having similar properties. This study revealed that the geomechanical properties of tunnel rocks are affected not only by in situ stresses but also by metamorphism affecting the rocks. The findings of this study can provide valuable reference data for addressing the evaluation of tunnel rocks especially for similar rock types in the eastern Black Sea Region where a lot of tunnel projects have been constructed.

## 5. Conclusions

In order to find out the effect of in-situ stress parameters and metamorphism on the geomechanical and mineralogical behavior of tunnel rocks, a series of laboratory tests on rock materials and field measurements on rock masses were performed. The following conclusions are drawn:

- In situ stress parameters (horizontal/vertical stress) were calculated as a function of depth and new correlations were tried to find out the effects of the depth factor on the geomechanical properties. High horizontal stress values obtained below 166 m depth affected the correlation relationships. Therefore, the relationships between the data pairs indicate more meaningful results ( $r = 0.77-0.88$ ) when the correlations were performed for the parameters obtained from depths higher than 166 meters.
- Findings of metabasalt obtained at the depth of 228 m were generally different from the others and showed more intense mineralization with varying sizes compared to other metabasalts. They are composed of nearly equal-sized microcrystals, providing a structure integrated with the rock.
- Mineralogical thin and polished section analyses revealed that low-grade contact metamorphism affected the basalts which were turned into metabasalts. Findings revealed that metabasalt obtained at the depth of 228 m was more affected by the increase in the grade of metamorphism.
- Consequently, the geomechanical properties of tunnel rocks are affected not only by in situ stresses but also by metamorphism affecting the rocks. Therefore, it is useful to evaluate these parameters in the design of underground structures such as tunnels.

## Acknowledgments

The author is grateful to Prof. Dr. Ayhan Kesimal, Prof. Dr. Bayram Ercikdi, and Assoc. Prof. Dr. Ferdi Cihangir for providing help during the laboratory studies, Assoc. Prof. Dr. Hasan Kolayli for the geological evaluation, and Geology Engineer Serkan Demirel for the field study.

## References

- Abioye, A.V. (2015), "Increasing effect of metamorphism on rock properties", *Int. J. Min. Sci. Technol.*, **25**(2), 205-211. <http://dx.doi.org/10.1016/j.ijmst.2015.02.007>.
- Abdou, M. and Mahmoud, A.N. (2013), "Correlation of sandstone rock properties obtained from field and laboratory tests", *Int. J. Civil Struct. Eng.*, **4**(1), 1-11.
- Anagnostou, G.A. (1993), "Model for swelling rock in tunneling", *Rock Mech. Rock Eng.*, **4**, 307-331. <https://doi.org/10.1007/BF01027115>.
- Banihashemigargari, E. and Rezaeifarei, A.H. (2023), "Mechanized tunnels lining prefabricated segments production methods", *Geomech. Eng.*, **32**(5), 503-512. <https://doi.org/10.12989/gae.2023.32.5.503>
- Barton, N.R. (2002), "Some new Q-value correlations to assist in site characterization and tunnel design", *Int. J. Rock Mech. Mining Sci.*, **39**(1), 185-216. [https://doi.org/10.1016/S1365-1609\(02\)00011-4](https://doi.org/10.1016/S1365-1609(02)00011-4)
- Barton, N., Lien, R. and Lunde, J. (1974), "Engineering classification of rock masses for the design of tunnel support", *Rock Mech.*, **6**, 189-239. <https://doi.org/10.1007/BF01239496>.
- Bieniawski, Z.T. (1989), "Engineering rock mass classifications. In: A complete manual for engineers and geologists in mining", Civil and Petroleum Engineering. Wiley, New York.
- Bieniawski, Z.T. (1989), "Engineering rock mass classifications", New York: Wiley
- Bird, J. (1942), "Rock bursts" – a symposium, AIME, Technical paper no: 1468. May.
- Brown, E.T. and Hoek, E. (1978), "Trends in relationships between measured in-situ stresses and depth", *Int. J. Rock Mech. Mining Sci., Geomech. Abs.*, **15**, 211-215.
- Bulut, F. and Tarhan, F. (1992), "Geomechanical properties of foundation rock of the Çambaşı (Trabzon-Çaykara) dam site (in Turkish)", *Geol. Eng.*, **41**, 138-145.
- Chen, C.H. Wang, T.T. Jeng, F.S. and Huang, T.H. (2012), "Mechanisms causing seismic damage of tunnels at different depths", *Tunn. Undergr. Sp. Tech.*, **28**, 31-40. <https://doi.org/10.1016/j.tust.2011.09.001>.
- Chen, L. Pei, W. Yang, Y. and Guo, W. (2022), "Three-dimensional numerical parametric study of shape effects on multiple tunnel interactions", *Geomech. Eng.*, **31**(3), 237-248. <https://doi.org/10.12989/gae.2022.31.3.237>.
- Chun, B.S., Ryu W.R., Sagong, M. and Do, J.N. (2009), "Indirect estimation of the rock deformation modulus based on polynomial and multiple regression analyses of the RMR system", *Int. J. Rock Mech. Mining Sci.*, **46**(3), 649-658. <https://doi.org/10.1016/j.ijrmm.2008.10.001>.
- Corkum, A.G., Damjanac, B. and Lam, T. (2018), "Variation of horizontal in situ stress with depth for long-term performance evaluation of the Deep Geological Repository project access shaft", *Int. J. Rock Mech. Mining Sci.*, **107**, 75-85. <https://doi.org/10.1016/j.ijrmm.2018.04.035>.
- Franklin, J.A. (1970), "Classification of rock according to its mechanical properties", Ph.D. Dissertation, University of London Imperial College, London, U.K

- Gurocak, Z. (2011), "Analyses of stability and support design for a diversion tunnel at the Kapikaya Dam Site, Turkey", *Bull. Eng. Geol. Env.*, **70**, 41-52. <https://doi.org/10.1007/s10064-009-0258-2>
- Herget, G. (1988), "Stresses in rock", Rotterdam: Balkema
- Hoek, E. and Diederichs, M.S. (2006), "Empirical estimation of rock mass modulus", *Int. J. Rock Mech. Min. Sci.*, **43**(2), 203-215. <https://doi.org/10.1016/j.ijrmms.2005.06.005>.
- ISRM. (2007), "The Complete ISRM Suggested Methods for Rock Characterization, Testing and Monitoring: 1974–2006", In: Ulusay, Hudson (Eds.), Suggested Methods Prepared by the Commission on Testing Methods, International Society for Rock Mechanics. ISRM Turkish National Group, Ankara, Turkey.
- Jiang, X.W., Wan, L., Wang, X.S., Liang, S.H.X. and Hu, B. (2009), "Estimation of fracture normal stiffness using a transmissivity-depth correlation", *Int. J. Rock Mech. Min. Sci.*, **46**(1), 51-58. <https://doi.org/10.1016/j.ijrmms.2008.03.007>.
- Kahraman, S. (2001), "Evaluation of simple methods for assessing the uniaxial compressive strength of rock", *Int. J. Rock Mech. Min. Sci.*, **38**(7), 981-994. [https://doi.org/10.1016/S1365-1609\(01\)00039-9](https://doi.org/10.1016/S1365-1609(01)00039-9).
- Kang, S.J., Lee, M., An, J.B., Lee, D.H. and Cho, G.C. (2023), "Dynamic behavior of submerged floating tunnels at the shore connection considering the use of flexible joints", *Geomech. Eng.*, **33**(1), 101-112. <https://doi.org/10.12989/gae.2023.33.1.101>.
- Karaman, K., Erçikdi, B. and Kesimal, A. (2013), "The assessment of slope stability and rock excavatability in a limestone quarry", *Earth Sci. Res. J.*, **17**(2), 169-181.
- Karaman, K. and Kesimal, A. (2015a), "Evaluation of the influence of porosity on the engineering properties of volcanic rocks from the Eastern Black Sea Region: NE Turkey", *Arab. J. Geosci.*, **8**, 557-564. <https://doi.org/10.1007/s12517-013-1217-6>.
- Karaman, K. and Kesimal, A. (2015b), "Correlation of Schmidt rebound hardness with uniaxial compressive strength and P-wave velocity of rock materials", *Arab. J. Sci. Eng.*, **40**, 1897-1906. <https://doi.org/10.1007/s13369-014-1510-z>.
- Karaman, K., Cihangir, F. and Kesimal, A. (2015), "A comparative assessment of rock mass deformation modulus", *Int. J. Min. Sci. Tech.*, **25**, 735-740. <http://dx.doi.org/10.1016/j.ijmst.2015.07.006>.
- Karaman, K. and Bakhytzhan, A. (2020), "Prediction of concrete strength from rock properties at the preliminary design stage", *Geomech. Eng.*, **23**(2), 115-125. <https://doi.org/10.12989/gae.2020.23.2.115>.
- Karaman, K., Alp, İ., Kesimal, A. and Yılmaz, A.O. (2019), "Investigation of the relationships between compressive strength and some physical parameters of pyrite containing rocks", *AKU-FEMUBID*, **19**(1), 248-255. <http://dx.doi.org/10.35414/akufemubid.476920>.
- Ketin, I. (1966), "Tectonic units of Anatolia", *Bull. Mineral Res. Exp. Ins. Turkey*, **66**, 22-34.
- Kim, J.W. Chong, S.H. and Cho, G.C. (2022), "Probabilistic Q-system for rock classification considering shear wave propagation in jointed rock mass", *Geomech. Eng.*, **30**(5), 449-460. <https://doi.org/10.12989/gae.2022.30.5.449>.
- Min, K.B., Rutqvist, J., Tsang, C.F. and Jing, L. (2004), "Stress-dependent permeability of fractured rock masses: A numerical study", *Int. J. Rock Mech. Min. Sci.*, **41**(7), 1191-1210. <https://doi.org/10.1016/j.ijrmms.2004.05.005>.
- Moomivand, H., Moosazadeh, S. and Gilani, S. (2022), "A new empirical approach to estimate the ratio of horizontal to vertical in-situ stress and evaluation of its effect on the stability analysis of underground spaces", *Rudarsko-Geološko-Naftni Zbornik*, **37**(3), 97-107. <https://doi.org/10.17794/rgn.2022.3.8>.
- Palmström, A. (1995), "RMi-A rock mass characterization system for rock engineering purposes", PhD. Thesis, University of Oslo, Norway.
- Parker, J. (1966), "Mining in a lateral stress field at White Pine", *Canadian Ins. Mining Metall. Trans.*, Vol. LXIX, 375-383.
- Sharma, S. and Judd, W.R. (1991), "Underground opening damage from earthquakes", *Eng. Geol.*, **30**(3-4), 263-276. [https://doi.org/10.1016/0013-7952\(91\)90063-Q](https://doi.org/10.1016/0013-7952(91)90063-Q).
- Sheorey, P.R. (1994), "A theory for in-situ stresses in isotropic and transversely isotropic rock", *Int. J. Rock Mech. Min. Sci. Geomech. Abs.*, **31**, 23 -34. [https://doi.org/10.1016/0148-9062\(94\)92312-4](https://doi.org/10.1016/0148-9062(94)92312-4).
- Singh, B., Goel, R.K., Jethwa, J.L. and Dude, A.K. (1997), "Support pressure assessment in arched underground openings through poor rock masses", *Eng. Geol.*, **48**(1-2), 59-81. [https://doi.org/10.1016/S0013-7952\(97\)81914-X](https://doi.org/10.1016/S0013-7952(97)81914-X).
- Sklyarov, E.V., Lavrenchuk, A.V., Fedorovsky, V.S., Gladkochub, D.P., Donskaya, T.V., Kotov, A.B., Mazukabzov, A.M. and Starikova, A.E. (2020), "Regional, contact metamorphism, and autometamorphism of the Olkhon Terrane (West Baikal Area)", *Petrology*, **28**, 47-61. <https://doi.org/10.1134/S0869591120010051>.
- Tugrul, A. and Zarif, I.H. (1999), "Correlation of mineralogical and textural characteristics with engineering properties of selected granitic rocks from Turkey", *Eng. Geol.*, **51**(4), 303-317. [https://doi.org/10.1016/S0013-7952\(98\)00071-4](https://doi.org/10.1016/S0013-7952(98)00071-4).
- Verman, M., Singh, B., Viladkar, M.N. and Jethwa, J.L. (1997), "Effect of tunnel depth on modulus of deformation of rock mass", *Rock Mech. Rock Eng.*, **30**(3), 121-127.
- Wang, X.S., Jiang, X.W., Wan, L., Song, G. and Xia, Q. (2009), "Evaluation of depth-dependent porosity and bulk modulus of a shear using permeability–depth trends", *Int. J. Rock Mech. Min. Sci.*, **46**, 1175-1181. <https://doi.org/10.1016/j.ijrmms.2009.02.002>.
- Yagiz, S. (2009), "Predicting uniaxial compressive strength, modulus of elasticity and index properties of rocks using the Schmidt hammer", *Bull. Eng. Geol. Environ.*, **68**, 55-63. <https://doi.org/10.1007/s10064-008-0172-z>.
- Yan, J., Cui, Y. and Liu, X. (2023), "Evolution of contact metamorphic rocks in the Zhoukoudian Area: evidence from phase equilibrium modelling", *Minerals*, **13**, 1056. <https://doi.org/10.3390/min13081056>.
- Zhao, Z., Jing, H., Shi, X., Yang, L., Yin, Q. and Gao, Y. (2021), "Study on bearing characteristic of rock mass with different structures: physical modeling", *Geomech. Eng.*, **25**(3), 179-194. <https://doi.org/10.12989/gae.2021.25.3.179>.
- Zhou, J. and Yang, X.A. (2021), "Deformation behavior analysis of tunnels opened in various rock mass grades conditions in China", *Geomech. Eng.*, **26**(2), 191-204. <https://doi.org/10.12989/gae.2021.26.2.191>.

GC